Journal of Statistical Physics, Vol. 62, Nos. 5/6, 1991

Theoretical Predictions of Diffusion from Brownian Motion in Superstrong Polymers

F. Dowell[1]

Received June 30, 1990; final October 25, 1990

This paper presents a summary of unique highly nonlinear static and dynamic theories for chain molecules (actually, for almost any kind of organic molecule), including the first superstrong polymers. These theories have been used to predict and explain (1) the physical self-assembly (self-ordering) of specific kinds of molecules into liquid crystalline (LC) phases (i.e., partially ordered phases) and (2) the diffusion of these molecules in various LC phases and the isotropic (*I*) liquid phase.

KEY WORDS: Dynamic properties; Brownian motion; diffusion; superstrong polymers; polymers; nonpolymeric molecules; liquid crystalline phases.

1. INTRODUCTION

This paper presents short summaries of highly nonlinear static and dynamic theories for complex organic molecules, including polymers. The dynamic theory uses forces and energies calculated from the static theory.

The dynamic theory is used to calculate diffusion from Brownian motion for nonpolymeric and polymeric molecules in pure states and in mixtures in the isotropic (*I*) liquid phase and in various liquid crystalline (LC) phases. The dynamic theory is also used to predict and explain diffusion from Brownian motion for superstrong liquid crystalline polymers (SS LCPs).

There is partial orientational ordering of the long axes of the molecules parallel to a preferred axis in the nematic (*N*) LC phase. In a

[1] Theoretical Division, Los Alamos National Laboratory, University of California, Los Alamos, New Mexico 87545.

0022-4715/91/0300-1059$06.50/0

smectic A (SA) LC phase, there is partial orientational ordering and partial one-dimensional (1D) positional ordering of the centers of mass of the molecules along the preferred axis, thus forming layered structures.

Polymer molecules are so long that they typically solidify too fast to order completely into the 3D crystalline state in sample sizes large enough for practical applications. The molecular ordering (and thus, strength) of a solid polymer can be significantly increased by solidifying the polymer from a LC phase. Backbone liquid crystalline polymers (LCPs) are polymers whose backbones have LC ordering; backbone LCP molecules have no side chains attached to the backbones. Strong polymers such as DuPont's Kevlar are solidified backbone LCPs and are used as stronger, lighter-weight replacements for metals, ceramics, and other materials in various structural applications, such as auto and airplane parts, armor, building materials, etc. Side-chain LCPs are polymers with relatively short non-polymeric side chains attached to the backbones, where the side chains have LC ordering. Combined LCPs are polymers whose backbones and side chains both have LC ordering.

Superstrong (SS) polymers[1-8] are *specially designed* combined LCPs in which the side chains of one molecule are designed to physically interdigitate (pack between) the side chains of neighboring molecules, thus leading to molecular self-reinforcement and enhanced mechanical properties (tensile strength, tensile modulus, and especially compressive strength) compared to backbone LCPs.

2. SUMMARY OF THEORIES

The theories in this paper are first-principles statistical physics theories. There are *no* ad hoc or arbitrarily adjustable parameters in the static theory or in the dynamic theory.

2.1. Summary of Static Theory

Since the static theory is derived and presented in detail in refs. 1 and 5–14, we present only a very short summary of the theory in this paper.

The static thermodynamic and molecular ordering properties of a system of molecules can be calculated using the configurational partition function Q_c of the system. To derive Q_c, the static theory[1,5-14] takes the continuum shape of a molecule; decomposes the shape into its x, y, and z components and maps these components onto a simple cubic lattice in a manner somewhat analogous to normal coordinate analysis in molecular spectroscopy; uses analytic lattice combinatorial statistics with a localized mean field approximation to calculate the packing and interactions of a

test molecule with all the other molecules in the system; and then takes various continuum limits. The lattice is used for mathematical tractability. The generalized lattice statistics used in the theory have been found to be very accurate (deviations less than 1%) compared[14,15] with Monte Carlo computer simulations in limiting cases presently amenable to such simulations. While conceptually simple, Q_c is algebraically very long and complex, since it contains so many details of the molecule chemical structures. Due to its extreme length, Q_c is not reproduced here; and the interested reader is referred to refs. 1 and 5–14 and references therein.

The change is made from a constant-volume V formulation to a constant-pressure P formulation. The pertinent variables in the partition function are then P, temperature T, system composition (i.e., mole fraction of each component present), and details of the molecule chemical structures [including bond lengths and angles, net energy differences E_g between *trans* and *gauche* intrachain rotational states, hydrogen bonds, dipole moments, bond polarizabilities, site–site Lennard-Jones (12, 6) potentials, degree of polymerization dp], and orientational and positional orderings of the different parts of the molecules. The molecular sites correspond to atoms or small groups of atoms, such as a benzene ring, a methylene group, an ester group, etc. Each interaction in the theory here depends explicitly on the intramolecular and intermolecular orientational and positional ordering of the specific molecular sites involved in the interaction. From the partition function, the PVT equation of state is then derived thermodynamically, as well as equations that minimize the Gibbs free energy of the system with respect to the average independent orientational and positional order variables of the different parts of the molecules.

There are *no* ad hoc or arbitrarily adjustable parameters in the theory. All variables used in the theory are taken from experimental data (such as bond lengths, bond angles, dipole moments, etc.) for atoms or small groups of atoms (such as benzene rings, methylene groups, etc.) or are calculated self-consistently using the theory.

The theory[1,5,7,13] has *predicted*, reproduced, and explained experimental trends in thermodynamic and molecular ordering properties such as phase transition temperatures, phase stabilities of N and multiple SA LC phases and of the I liquid phase, orientational order P_2, parallel and perpendicular radii of gyration, volumes, and odd–even effects for various backbone LCPs, side-chain LCPs, nonpolymeric LC materials, non-LC polymers, and mixtures of these materials as a function of T, P, system composition, and molecule chemical structure. Odd–even effects are alternations in the magnitudes of various thermodynamic and molecular ordering properties as the number of carbon atoms in an n-alkyl chain varies from odd to even.

The theory has given[1,5,7-9] very good quantitative *predictive* and reproductive agreement (relative deviations between 0% and less than about 6.4%) with available experimental data for these properties. These above comparisons were performed for various backbone LCPs (such as Kevlar-type LCPs and polyesters), various side-chain LCPs (such as polymethacrylates and polymethylsiloxanes), and nonpolymeric LC materials [(such as *p*-azoxyanisole (PAA)].

This static theory is unique in relating all the above properties to T, P, and specific molecule chemical structures.

2.2. Dynamic Theory

Here is summarized a recent new dynamic theory[6-8] for Brownian motion and diffusion for almost any organic polymeric or nonpolymeric molecule in the isotropic (I) liquid phase and in various LC phases. The diffusion of the molecules constitutes a lower limit (i.e., slowest rate) for the speed at which a material can be processed.

Earlier theoretical treatments (see, for example, reviews in refs. 16 and 17) of diffusion and other dynamic properties have treated simple generalized systems such as the case of dumbbells[16] in a generalized field or the case of generalized chains repeating[17] in a tube representing a generalized field.

In contrast, the new theory here is the first theory to calculate diffusion coefficients as a function of the *specific* molecule chemical structures, T, and P.

The basic idea of this new dynamic theory is to use the site–site intermolecular energies and forces from the static theory summarized earlier to calculate friction coefficients, etc., for analytic Brownian motion calculations for the molecules. From refs. 18 and 19, the aperiodic case of Brownian motion of a harmonically-bound particle is given by

$$x_b^2 = H_1 + (x_{b0}^2 - H_1)[1 + (H_2/2)]^2 \exp(-H_2) \tag{1}$$

where

$$H_1 = k_B T/(m_b \omega_b^2) \tag{2}$$

$$H_2 = \beta t \tag{3}$$

$$\beta = f_b/m_b \tag{4}$$

where t is the time, x_b is the average position at time t, x_{b0} is the position at time $t=0$, m_b is the mass of the particle, ω_b is the frequency of the particle (in 2π), f_b is the friction coefficient, and k_B is the Boltzmann constant.

In the theory here, m_b is assigned to be the mass of the entire molecule, and ω_b to be the average frequency of the largest rigid vibrating parts in the molecule. The rationale for these assignments is as follows: Focus on the largest rigid vibrating parts of the molecules, since these are the parts of the molecules that will be moving the slowest and thus will most limit the degree of motion and the rate of diffusion. The largest rigid vibrating parts undergo random vibrations with respect to other parts of the molecule; these vibrations are somewhat decoupled from each other by semiflexible bonds in the molecule. However, the largest rigid vibrating parts must drag the mass of the entire molecule with them. There is one largest rigid vibrating part of each k-type packing, where $k = 1$ refers to the packing of the backbones of molecules, while $k = 2$ and $k = 3$ refer to the packing of the side chains of molecules. For more discussion of these k designations, see the static theory in refs. 1 and 5–9. The friction coefficient f_b is given by

$$f_b = F_b / v_b \tag{5}$$

where F_b is the average intermolecular force acting on the largest rigid vibrating parts, and v_b is the average velocity of the largest rigid vibrating parts. The velocity v_b is calculated by equating the kinetic energy of the molecule to the potential energy U of the largest rigid vibrating parts:

$$m_b v_b^2 / 2 = U \tag{6}$$

where

$$U = \frac{\sum_k \left[m_k \left(\sum_{y,z} \omega_{yzk} \right) \right]}{\sum m_k} \tag{7}$$

$$F_b = \frac{\sum_k \left\{ m_k \left[\sum_{y,z} (\partial \omega_{yzk} / \partial a_k) \right] \right\}}{\sum m_k} \tag{8}$$

and $\sum_k \omega_{yzk}$ is the sum of all site–site intermolecular potential energies for the largest rigid vibrating parts in all the k-type packings.

The m_k represent the number of molecular segments in a backbone repeat unit for $k = 1$ and in a side chain for $k = 2$ or 3. Also, ω_{yzk} is the intermolecular interaction energy between a segment y and a segment involved in k-type packing. Each ω_{yzk} includes explicit (1) Lennard-Jones (12, 6) potentials for repulsive interactions and London dispersion (van der Waals) attractive interactions, (2) dipole/dipole interactions, (3) dipole/induced dipole interactions, and (4) hydrogen bonding. a_k is the average separation distance between first-neighbor intermolecular segments

involved in k-type packing. ω_{yzk}, a_k, and m_k are calculated in the static theory (see refs. 1 and 5–9).

Note that U and F_b are calculated from the intermolecular potential energies ω_{yzk} and separation distances a_k, which are calculated in the static theory for the phase of lowest free energy as a function of T, P, system composition, and molecule chemical structures. Thus, U and F_b are determined by the details of the molecule chemical structures and the orientational and positional ordering of the molecules. Also,

$$\omega_b^2 x_b = F_b/m_b \tag{9}$$

from the harmonic oscillator equation. It should be noted that the forces and energies are calculated in the static theory from anharmonic potentials; thus, these forces and energies introduce anharmonicity into Eq. (1).

Equation (1) is then solved for x_b. Let t_a be the smallest value of the time t at which the value of x_b has increased to its maximum value x_{ba}, within the precision desired for t_a and thus for the diffusion coefficient calculated later from t_a. Thus, t_a is the minimum time required to reach the maximum displacement x_{ba}, within the precision desired for t_a. One can calculate x_{ba} from Eqs. (1) and (9) by setting $t = \infty$. Specifically, from Eqs. (1) and (9),

$$x_{ba}^2 = H_1 = \frac{k_B T}{m_b \omega_b^2} \qquad \text{for} \quad t = \infty \tag{10}$$

and

$$x_{ba} = k_B T / F_b \qquad \text{for} \quad t = \infty \tag{11}$$

However, Eqs. (10) and (11) do not contain t as a variable and thus cannot be used to calculate t_a directly. In practice, t_a is determined by increasing t until $x_b \to x_{ba}$ and thus any further increase in t does not increase the value of x_b, within the precision desired for t_a. The time t is increased using as an increment the degree of precision desired in t_a. In this paper as in refs. 6–8, t_a was calculated to the nearest third significant figure, since three significant figures constituted the largest number of significant figures in the available experimental data for diffusion coefficients referenced in this paper and in earlier papers[6-8] using this theory. The macroscopic diffusion coefficient D_b is given by

$$D_b = x_{ba}^2 / t_a \tag{12}$$

2.3. Agreement of Dynamic Theory with Experiment

This dynamic theory reproduces the experimental trends in diffusion coefficients for polymeric and nonpolymeric molecules in the pure state or

Table I. Theoretical and Experimental Values of the Diffusion Coefficient D_{b0} of the Non-LC Backbone Polymer Polyisoprene at Infinite Dilution in Hexane at Different Molecular Weights of the Polymer at $T = 293$ K[a]

Molecular weight ($\times 10^4$)	D_{b0} ($\times 10^{-7}$ cm^2 sec^{-1})	
	Theoretical	Experimental
27	2.93	3
166	1.13	1.01

[a] The phase is the *I* liquid phase. The experimental data are from ref. 20.

in binary mixtures as a function of T, P, and molecule chemical structure. This theory also gives good quantitative agreement with available experimental data for these properties. For example, Table I shows the good agreement[6-8] between the results from this theory and the experimental results[20] for the diffusion coefficient of the non-LC backbone polymer polyisoprene at different molecular weights at infinite dilution in hexane [$CH_3-(CH_2)_4-CH_3$] in the *I* liquid phase at $T = 293$ K. Also, for example, Table II shows the good agreement[6-8] between the results from this theory and the experimental results[21] for the self-diffusion coefficient for the nonpolymeric LC material PAA in the *N* LC phase at $T = 400$ K. For the PAA molecule, the largest rigid vibrating part is $O-\phi-(NO)=N-\phi-O$, where ϕ is a *para*-bonded phenyl group. This largest rigid vibrating part is used in the theory to calculate D_b. In the above calculations, $P = 1$ atm. See Fig. 1 for the molecule chemical structures of polyisoprene and PAA. Note also that there is some uncertainty in the experimental diffusion coefficients.

Table II. Theoretical and Experimental Values of the Self-Diffusion Coefficient D_b for the Nonpolymeric LC Material PAA in the *N* LC Phase at $T = 400$ K[a]

T (K)	D_b ($\times 10^{-6}$ cm^2 sec^{-1})	
	Theoretical	Experimental
400	3.47	~3.4

[a] The experimental data are from ref. 21.

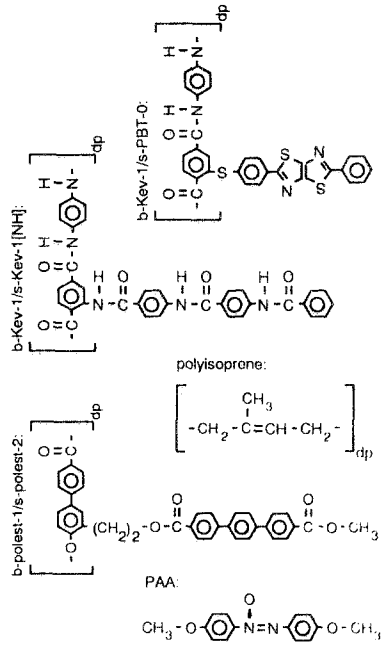

Fig. 1. Molecule chemical structures of the theoretically-designed candidate SS LCPs *b*-Kev-1/*s*-PBT-O, *b*-Kev-1/*s*-Kev-1[NH], and *b*-polest-1/*s*-polest-2; of the non-LC polymer polyisoprene; and of the nonpolymeric LC PAA.

3. PREDICTIONS FOR DIFFUSION OF CANDIDATE SS LCP MOLECULES

In earlier papers,[1-8] the static theory was used to predict and design (atom by atom, bond by bond) the first candidate SS LCPs and to predict many of their static properties. SS LCPs are combined LCPs designed such that the state of lowest free energy is the state in which the side chains of one molecule physically interdigitate with the side chains of neighboring molecules, as shown in Fig. 2a. The interdigitation of the side chains keeps the molecules from being pushed past each other or peeled apart and is thus the origin of the good compressive strength. Since the molecules are not chemically cross-linked, these SS LCPs are designed to be easy to process and reprocess. Some SS LCPs have been designed[1-8] with side chains that pack on alternating sides of the backbones (see Fig. 2a–2c), and some SS LCPs (such as those discussed later in the paper) have been designed with side chains that pack on one side of the backbone (see Fig. 2d).

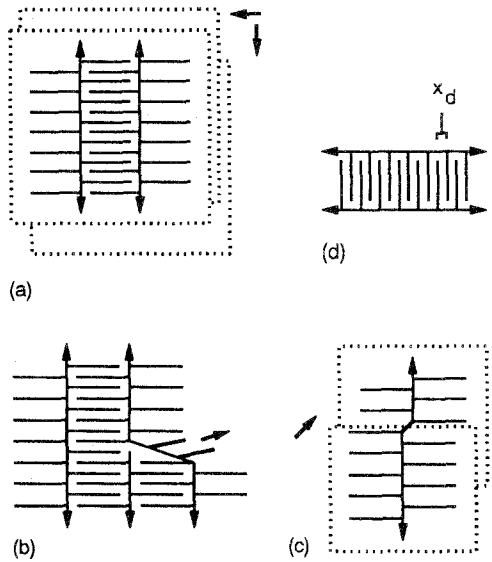

Fig. 2. *Schematic* illustrations: The solid lines represent the long axes of the side chains and the backbones of the SS LCP molecules, where these side chains and backbones can have both rigid and semiflexible sections; the continuation of the backbones is indicated by the small arrows. (a) Packing of SS LCPs in planes (denoted with dotted lines); the diffusion of a molecule in a plane between the planes of other molecules is indicated by the bold arrows. (b, c) Small defects in the packing of the SS LCP molecules generate effective long-range 3D LC ordering; the bold arrows and bold molecular parts indicate packing in the third dimension. (d) Spacing distance x_d (along the backbone) between interdigitated side chains of SS LCP molecules.

Research on the chemical synthesis of several of these theoretically-designed SS LCPs is in progress at multiple research institutions.

The static theory predicts[18] that the backbones and side chains of SS LCPs tend to physically pack in planes, such that backbones tend to orientationally order with other backbones in the same plane, and similarly for side chains. There is thus *N* LC ordering of the backbones *in* a plane and also *local* interdigitated SA LC ordering of side chains *in* a plane. There is also orientational ordering (alignment) of planes, such that backbones in one plane orientationally align with backbones in other planes, and similarly for side chains. There is thus *N* LC ordering of the planes in three dimensions (3D). At finite temperatures, small, naturally occurring defects in the packing of the molecules lead to an effective long-range 3D LC orientational and positional ordering of the molecules and thus to effective long-range 3D strength in the system (see Figs. 2b and 2c.)

Table III. Theoretical Values of the Side-Chain P_2 and the D_b of SS LCPs That are Scaled Versions of *b*-polest-1/*s*-polest-2 at $dp = 100$ and $T = 400$ K

r_d	x_d (Å)	Side-Chain P_2	D_b ($\times 10^{-6}$ cm^2 sec^{-1})
1.000	5.32	0.886	2.56
0.846	4.50	0.980	0.14

In the following results, the calculated values of various properties are those values for the SS LCPs in the limit of removal of the least drop of solvent just before forming a polymer solid (glass) at the indicated T and at $P = 1$ atm.

3.1. Opposing Trends in Strength vs. Processability Limits for SS LCPs

Table III shows how the side-chain orientational order variable P_2 and diffusion coefficient D_b of the theoretically-designed candidate SS LCP *b*-polest-1/*s*-polest-2 (see Fig. 1) varies[6-8] as the interdigited side-chain spacing distance x_d (see Fig. 2d) is varied along the backbone of the SS LCP. P_2 is calculated using the static theory, and D_b using the dynamic theory (with input from the static theory),

$$P_2 = \langle 3 \cos^2 \theta_k - 1 \rangle / 2 \tag{13}$$

where θ_k is the angle between the long axis of the side chain and the preferred axis of orientation for the side-chain long axis. One has $0 \leqslant P_2 \leqslant 1$; $P_2 = 0$ indicates no order; $P_2 = 1$ indicates full orientational order.

To isolate the effect of verying x_d in Table III from the effects of different molecule chemical structures, we start with the SS LCP structure

Table IV. Theoretical Values of D_b vs. T for the SS LCP *b*-Kev-1/*s*-PBT-O at $dp = 1000$

Superstrong LCP	T (K)	D_b ($\times 10^{-7}$ cm^2 sec^{-1})
b-Kev-1/*s*-PBT-O	300	2.86
	600	10.1

Table V. Theoretical Values of D_b vs. Side-Chain Length for SS LCPs at $dp = 1000$ and $T = 600$ K

Superstrong LCP	Side-chain length (Å)	D_b ($\times 10^{-7}$ cm^2 sec^{-1})
b-Kev-1/*s*-PBT-O	14.89	10.1
b-Kev-1/*s*-Kev-1[NH]	20.74	4.82

b-polest-1/*s*-polest-2 with $dp = 100$ at $T = 400$ K and $P = 1$ atm. Then, we scale the length of the repeat unit along the backbone, all intermolecular interactions, etc., of *b*-polest-1/*s*-polest-2 by the ratio r_d of a new interdigitated side-chain separation distance x_{di} to the original interdigitated side-chain separation distance x_{d1}.

Recall that diffusion constitutes the lower limit (i.e., slowest rate of molecular rearrangement) for processability. As x_d decreases in Table III, the side-chain P_2 (and thus, the compressive strength) increases, but the diffusion coefficient D_b decreases, that is, the SS LCP molecules are slower to rearrange and thus the SS LCP is harder to process. Thus, as x_d varies, there are opposing trends in (1) side-chain ordering (thus, compressive strength) and (2) diffusion coefficient (thus, ease of molecular rearrangement for processing). That is, the compressive strength is increased at the expense of the ease of molecular rearrangement needed for processing. The theoretically-designed candidate SS LCPs in this paper and earlier papers[1-8] have been designed to optimize the conflicting trends in these two goals.

3.2. Other Trends in Diffusion Coefficients for SS LCPs

Tables IV–VI show the theoretical calculations for the diffusion coefficient D_b as a function of T, side-chain length, and dp for two other

Table VI. Theoretical Values of D_b vs. dp for the SS LCP *b*-Kev-1/*s*-Kev-1[NH] at $T = 600$ K

Superstrong LCP	dp	D_b ($\times 10^{-7}$ cm^2 sec^{-1})
b-Kev-1/*s*-Kev-1[NH]	10	50.5
	100	16.2
	1000	4.82

theoretically-designed candidate SS LCPs, *b*-Kev-1/*s*-Kev-1[NH] and *b*-Kev-1/*s*-PBT-O (see Fig. 1).

As expected, the diffusion of SS LCPs is faster at higher T, as shown in Table IV.

As expected, the diffusion of SS LCPs is faster for shorter side chains, as shown in Table V.

As expected, the diffusion of SS LCPs is faster at smaller dp, as shown in Table VI. That is, the SS LCP with the shorter backbone diffuses faster.

Note that although there is considerable variation in the magnitudes of the diffusion coefficients for the SS LCPs in Tables III–VI, the diffusion coefficients for these SS LCPs are reasonable compared with the diffusion coefficients for existing nonpolymeric LC molecules and non-LC polymeric molecules (see, for example, Tables I and II).

The calculations[6-8] with this dynamic theory also predict that a SS LCP molecule diffuses faster when it diffuses in a plane between (and parallel to) the planes of the other molecules, as indicated in Fig. 2a.

ACKNOWLEDGMENTS

This research was supported by the U. S. Department of Energy, Office of Basic Energy Science, Division of Materials Sciences.

REFERENCES

1. F. Dowell, *J. Chem. Phys.* **91**:1316 (1989).
2. F. Dowell, *J. Chem. Phys.* **91**:1326 (1989).
3. F. Dowell, *Polymer Preprints* **30**(2):532 (1989).
4. F. Dowell, in *Industry–University Advanced Materials Conference II*, F. W. Smith, ed. (Advanced Materials Institute, Colorado School of Mines, Golden, Colorado, 1989), p. 605.
5. F. Dowell, *Mat. Res. Soc. Symp. Proc.* **134**:33 (1989).
6. F. Dowell, *Nonlinear Structures in Physical Systems*, L. Lam and H. C. Morris, eds. (Springer-Verlag, New York, 1990), p. 232.
7. F. Dowell, in *Liquid Crystalline Polymers*, R. A. Weiss and C. K. Ober, eds. (American Chemical Society, Washington, D.C., 1990), p. 335.
8. F. Dowell, *Adv. Chem. Phys.* (in press).
9. F. Dowell, *Mat. Res. Soc. Symp. Proc.* **134**:47 (1989).
10. F. Dowell, *Phys. Rev. A* **38**:382 (1988); **36**:5046 (1987).
11. F. Dowell, *Mol. Cryst. Liq. Cryst.* **157**:203 (1988); **155**:457 (1988).
12. F. Dowell, in *Competing Interactions and Microstructures: Statics and Dynamics*, R. LeSar, A. Bishop, and R. Heffner, eds. (Springer-Verlag, Berlin, 1988), p. 117.
13. F. Dowell, *Phys. Rev. A* **31**:2464, 3214 (1985); **28**:3526 (1983).
14. F. Dowell, *Phys. Rev. A* **28**:3520 (1983).
15. F. L. McCrackin, *J. Chem. Phys.* **69**:5419 (1978).

16. R. Bird, C. I. Curtiss, R. C. Armstrong, and O. Hassager, *Dynamics of Polymer Liquids: 2. Kinetic Theory* (Wiley, New York, 1987).
17. M. Doi and S. F. Edwards, *The Theory of Polymer Dynamics* (Oxford University Press, Oxford, 1986).
18. G. E. Uhlenbeck and L. S. Ornstein, *Phys. Rev.* **36**:823 (1930).
19. S. Chandrasekhar, *Rev. Mod. Phys.* **15**:1 (1943).
20. J. Brandrup and E. H. Immergut, eds., *Polymer Handbook*, 2nd ed. (Wiley, New York, 1975), p. IV-68.
21. G. J. Kruger, *Phys. Rep.* **82**:230 (1982).